Biochemical characterization of phosphoserine phosphatase SerB2 from Mycobacterium marinum

Pierson, Elise; Wouters, Johan

Published in:
Biochemical and Biophysical Research Communications

DOI:
https://doi.org/10.1016/j.bbrc.2020.07.017

Publication date:
2020

Document Version
Peer reviewed version

Biochemical characterization of phosphoserine phosphatase SerB2 from *Mycobacterium marinum*

Elise Pierson* and Johan Wouters

Laboratoire de Chimie Biologique Structurale (CBS), Namur Medicine and Drug Innovation Center (NAMEDIC), Namur Research Institute for Life Sciences (NARILIS), University of Namur (UNamur), B-5000 Namur, Belgium

* Corresponding author at Laboratoire de Chimie Biologique Structurale (CBS), Namur Medicine and Drug Innovation Center (NAMEDIC), Namur Research Institute for Life Sciences (NARILIS), University of Namur (UNamur), Rue de Bruxelles 61, B-5000 Namur, Belgium

Phone: +32 (0)81 72 45 69

E-mail: elise.pierson@unamur.be

ABSTRACT

SerB2 is an essential phosphoserine phosphatase (PSP) that has been shown to be involved in *Mycobacterium tuberculosis* (*Mtb*) immune evasion mechanisms, and a drug target for the development of new antitubercular agents. A highly similar (91.0 %) orthologous enzyme exists in the surrogate organism *Mycobacterium marinum* (*Mma*) and could have acquired similar properties. By homology modeling, we show that the two PSPs are expected to exhibit almost identical architectures. *Mma*SerB2 folds into a homodimer formed by two intertwined subunits including two ACT regulatory domains followed by a catalytic core typical of HAD (haloacid dehalogenase) phosphatases. Their *in vitro* catalytic properties are closely related as *Mma*SerB2 also depends on Mg^{2+} for the dephosphorylation of its substrate, *O*-phospho-L-serine (PS), and is most active at neutral pH and temperatures around 40°C. Moreover, an enzyme kinetics study revealed that the enzyme is inhibited by PS as well, but at lower concentrations than *Mtb*SerB2. Substrate inhibition could occur through the binding of PS in the second active site and/or at the ACT domains interface. Finally, previously described beta-carboline *Mtb*SerB2 inhibitors also decrease the phosphatase activity of *Mma*SerB2. Altogether, these results provide useful information when *M.marinum* is used as a model to study immune evasion in tuberculosis.

KEYWORDS

Mycobacterium marinum, SerB2, phosphoserine phosphatase, HAD phosphatases, clofazimine, harmine derivatives

ABBREVIATIONS[1]

[1] CFZ, clofazimine ; HAD, haloacid dehalogenase ; *Mma*, *Mycobacterium marinum* ; *Mtb*, *Mycobacterium tuberculosis* ; PGDH, phosphoglycerate dehydrogenase ; P_i, inorganic phosphate ; PS, *O*-phospho-L-serine ; PSAT, phosphoserine aminotransferase ; PSP, phosphoserine phosphatase

INTRODUCTION

Mycobacterium marinum (Mma) is a free-living nontuberculous mycobacterium found worldwide in fresh-, salt- and brackish water [1]. The organism mostly causes tuberculosis-like infection in fish and amphibians but can also infect humans by entering the skin through superficial wounds [2,3]. Within a few weeks after exposure, infected individuals develop purulent granulomatous skin lesions at the site of the inoculation (usually the hands) [4,5]. The disease is known as the "fish tank granuloma" and, even if quite rare, is a risk for anyone handling fish or exposed to improperly chlorinated waters [6]. Outbreaks of *M. marinum* can, therefore, be a major concern for zebrafish research facilities, both in terms of staff and fish [7].

Because of the similarities in the pathologies they cause and their very close genetic relatedness, *M. marinum* has been widely used as a surrogate organism for *M. tuberculosis (Mtb)* and model to study the pathogenesis of tuberculosis in humans [8–12]. The two macrophage pathogens share over 3000 orthologous genes with an average amino acid identity of 85% and very similar genetic programs in terms of virulence and protection [13,14]. Moreover, the classification of *M. marinum* as a BSL2 organism and its comparatively rapid growth make it easier to manipulate in the laboratory than its counterpart [15].

Most organisms synthesize L-serine *de novo* via the so-called "phosphorylated pathway". In this biosynthetic route, a phosphoglycerate dehydrogenase (PGDH EC 1.1.1.95) first converts the glycolytic intermediate 3-phosphoglycerate to 3-phosphohydroxypyruvate, which is in turn transformed to *O*-phospho-L-serine (PS) by a phosphoserine aminotransferase (PSAT, EC 2.6.1.52). The third and last step then involves a phosphoserine phosphatase (PSP, EC 3.1.3.3) that catalyzes the irreversible dephosphorylation of PS to give L-serine. [16,17] In *M.*

tuberculosis, the three enzymes are respectively encoded by the essential genes *serA1*, *serC*, and *serB2* [18,19]. While *Mtb*PGDH SerA1 and *Mtb*PSAT SerC appear to play a purely metabolic role, *Mtb*PSP SerB2 also acts as an effector protein in infected macrophages [20,21]. As demonstrated by Shree *et al.* [21], the interaction of *Mtb*SerB2 with various host proteins elicits cytoskeleton rearrangements, inhibition of apoptotic pathways, and down-regulation of inflammatory cytokine IL-8. These effects are reversed by Clofazimine (CFZ), a riminophenazine drug that inhibits *Mtb*SerB2 phosphatase activity. Several other *Mtb*SerB2 inhibitors have been identified by various groups, including ours, thereby confirming the druggability of the enzyme [22–24]. *Mtb*SerB2 is now considered a promising therapeutic target for the treatment of tuberculosis, which continues to be a major public health issue.

Given the very close genetic relationship between the two pathogens, it is not surprising that *M. marinum* also possesses the enzymes of the phosphorylated pathway [13]. The orthologous PSPs exhibit a high sequence similarity (91.0 %) and it could be possible that *Mma*SerB2 has also gained effector functions allowing the modulation of host immune response. In this work, we report for the first time a biochemical characterization of *Mma*SerB2 and a comparison with its close homolog *Mtb*SerB2.

MATERIALS AND METHODS

In silico analysis tools

Multiple sequence alignment was obtained using MultAlin [25] and the related figure was prepared using ESPript 3.0 [26]. Sequence identity values were calculated using the Sequence Manipulation Suite [27]. The figures of the 3D model were prepared using PyMOL Molecular Graphics System.

Expression and purification of *Mma*SerB2

Escherichia coli strain BL21 (DE3) was transformed with a pAVA0421 plasmid encoding for an N-terminal His_6-tagged *Mma*SerB2 under control of the T7 RNA polymerase promoter. The plasmid contains the ampicillin resistance gene (*ampR*). Protein expression and purification were carried as described in reference [24]. The concentration of the tagged protein was determined spectrophotometrically at 280 nm using 11585 M^{-1} cm^{-1} as the extinction coefficient and 45.83 kDa as the molar mass.

Enzymatic activity assay, inhibition, and kinetics studies

Enzyme activity was measured in an end-point phosphatase assay, using malachite green and ammonium heptamolybdate at low pH to colorimetrically determine the amount of inorganic phosphate (P_i) released during the hydrolysis of PS. Reactions were carried with 0.2 mM PS in Tris-HCl buffer according to the standard test conditions and protocol detailed in reference [24]. The standard test buffer (pH or 5 mM metal ion as chloride salt) or temperature of the assay were varied in order to study each parameter independently. For native kinetics measurements, 200 µL-reactions containing 1 pmol enzyme and 0 to 7.5 mM PS in standard test buffer were allowed to proceed for 10 min at 37°C. Initial velocities were reported as the amount of P_i released per microgram of enzyme per minute. For inhibition assays, reactions were carried with 0.4 mM PS, 2% DMSO and 0 (DMSO control), 10, or 100 µM inhibitor.

Evaluation of kinetic parameters

The kinetic parameters of *Mma*SerB2 were determined by fitting the model described by LiCata and Allewell [28] to the experimental velocity curves. This model (**equation (1)**), based on a modified Hill equation, accounts for cooperative substrate binding as well as partial uncompetitive substrate inhibition:

$$v = \frac{V_{max} + V_i\left(\frac{[S]}{K_i}\right)^x}{1 + \left(\frac{K_M}{[S]}\right)^n + \left(\frac{[S]}{K_i}\right)^x} \qquad (1)$$

v is the initial velocity (nmol µg^{-1} min^{-1}) at substrate concentration [S] (mM), V_{max} is the maximal velocity (nmol µg^{-1} min^{-1}), K_M is the Michaelis-Menten constant (mM), V_i is the final velocity at infinite substrate concentration (nmol µg^{-1} min^{-1}), K_i is the substrate inhibition constant (mM) representing the concentration of inhibitor (substrate) required to decrease V_{max} by half, *n* is the Hill coefficient reflecting cooperativity in substrate binding and *x* is another Hill coefficient taking into account that substrate inhibition may also be cooperative. The value of *x* must be fixed to obtain convergence. We have empirically determined the value of *x* giving the best fit. The smallest standard error of the estimate was obtained with $x = 5$. The values of V_{max}, V_i, K_M, K_i, and *n* were calculated by non-linear regression based on **equation (1)** using GraphPad Prism 6 (GraphPad Software, La Jolla California USA).

RESULTS AND DISCUSSION

In silico analysis of *Mma*SerB2

The phosphoserine phosphatase SerB2 from the M strain of *M. marinum* (UniProt accession number B2HHH0) has a length of 411 aa and a mass of 43443 Da. Two other genes designated as *serB* and *serB1* in the genome of the M strain are also listed as PSPs in the ENA database (accession numbers ACC43554.1 and ACC39293.1). The gene products *Mma*SerB (285 aa) and *Mma*SerB1 (303 aa) are shorter and share respectively 23.1 % and 29.8 % sequence similarity with *Mma*SerB2, and 48.4 % similarity among themselves. Transposon mutagenesis experiments have identified *Mma*SerB1 as most likely essential for the survival of *M. marinum* strain E11 [29] while its *M. tuberculosis* H37Rv orthologue *Mtb*SerB1 is not [18]. The only essential PSP in *M. tuberculosis* H37Rv is *Mtb*SerB2 with

which *Mma*SerB2 shares 91.0 % similarity and 85.9 % identity. A Pfam search confirmed that *Mma*SerB2, like *Mtb*SerB2, is a haloacid dehalogenase (HAD)-like hydrolase that possesses 2 extra N-terminal ACT domains (Pfam 13740 and 01842). These domains, found in some PSPs only, are known to regulate enzyme activity by binding amino acids [30,31]. The multiple sequence alignment shown in **Figure 1** illustrates the high similarity of mycobacterial PSPs and highlights the presence of the 4 signature motifs of HAD phosphatases in *Mma*SerB2 [32,33]. The ACT domains, absent in human PSP, are also highly conserved and all residues that are known to be important for binding of L-serine in *Mtb*SerB2 [22,34] and SerB from *M. avium* (*Mav*SerB, based on the surrounding residues in PDB structures 5JLR and 5JLP) are present in *Mma*SerB2. *Mav*SerB (PDB 3P96, 83.4% sequence identity) was employed as a template to model the 3D structure of *Mma*SerB2 using SWISS-MODEL [35]. As expected, the homology model (**Figure 2A**) exhibited three distinct domains: the catalytic core, arranging into a Rossmannoid fold typical of HAD phosphatases topped with a C1 cap module [32], and two α/β sandwiches forming the ACT domains, connected by a loop of about 10 aa. *Mma*SerB2 is also predicted to be a homodimer, in which the monomeric subunits swap their N-terminal ACT domain (**Figure 2B**). The superimposition of *Mma*SerB2 model with the structures of *Mav*SerB 3P96 and *Mtb*SerB2 modeled in the same way led to root mean square deviations of 0.103 and 0.057 Å, respectively. These results confirm that the three enzymes are expected to share almost identical architectures. According to the models, all the residues that differ between *Mma*SerB2 and *Mtb*SerB2 are found at the surface, and the organization of the active site is perfectly conserved (**Figure S1**).

Effects of selected metal cations, pH and temperature on *Mma*SerB2 activity

The phosphatase activity of *Mma*SerB2 was measured at pH 7.4 and 37°C in the presence of Mg^{2+}, Mn^{2+}, Ca^{2+}, Cu^{2+}, Fe^{3+}, Ni^{2+}, and Zn^{2+} at 5 mM, and in a metal ion-free buffer. As

shown in **Figure 3A**, *Mma*SerB2 activity was significantly different from zero only in the presence of Mg^{2+}, Mn^{2+}, or Ca^{2+}. The highest activity was observed in presence of Mg^{2+} and the activities in the presence of Mn^{2+} and Ca^{2+} were respectively 37% and 7% of that seen with Mg^{2+}. The same trend is reported for *Mtb*SerB2 [22,23]. Together with the fact that the enzyme was inactive in the metal ion-free buffer, these results indicate that *Mma*SerB2 is dependent on divalent metal cations and most certainly uses Mg^{2+} as an obligatory cofactor. This observation is a common feature of all HAD phosphatases [32].

The pH dependence of *Mma*SerB2 phosphatase activity in Tris-HCl buffer at pH values ranging from 7.0 to 9.0 and 37°C is shown in **Figure 3B**. The optimum pH for the dephosphorylation of PS was observed around 7.6, with the enzyme showing 92% and 98% of its maximum activity at pH 7.4 and 7.8, respectively. The enzyme was active over the entire tested pH range with relative activities over 70% at pH 7.0 and pH 8.2. Beyond this pH value, the activity decreased almost linearly to reach 44% relative activity at pH 9.0. These results are in line with the findings published earlier for *Mtb*SerB2 [22,23].

The optimal temperature for *Mma*SerB2 phosphatase activity was investigated in the range 25-60°C. As shown in **Figure 3C**, the optimal temperature was found to be 42°C. At 25°C, the enzyme showed 46% of its maximum activity. The enzymatic activity increased with the reaction temperature up to 42°C, a ten degree rise in temperature almost doubling the activity. The temperature range in which *Mma*SerB2 was most active (over 80% relative activity) extended from 34 to 44°C. Above 50°C, the activity decreased sharply with the reaction temperature. The enzyme showed only 6% relative activity at 54°C and was totally inactive at 60°C. Comparatively, the optimal temperature described by Yadav, Shree *et al.* for *Mtb*SerB2 is 37°C but no activity values were reported between 40 and 50°C in their work [15]. Nevertheless, the effect of temperature on the hydrolytic activities of the two enzymes is similar.

Kinetic characterization of native *Mma*SerB2

To evaluate the kinetic properties of *Mma*SerB2, its phosphatase activity was measured at PS concentrations ranging from 0 to 7.5 mM. The plot of initial velocity against PS concentration is shown in **Figure 3D**. The shape of the curve clearly indicated partial inhibition by the substrate above a concentration of 3 mM, as the velocity increased to a maximum and then decreased to a plateau. This observation was not surprising since Grant demonstrated that the orthologous *Mtb*SerB2 is also inhibited by PS using a similar assay [34]. The usual kinetic parameters were derived from fitting **equation (1)** to the experimental data and reported in **Table 1**, along with *Mtb*SerB2 kinetic parameters from other work for comparison [24,34]. While k_{cat} values were of the same order of magnitude for both enzymes, the K_M value was 2.6 to 5 times higher for *Mma*SerB2. This observation could mean that the latter enzyme is somewhat less affine for PS than its *Mtb* ortholog. The parameters n, K_i and V_i were also calculated for *Mma*SerB2. The inhibited rate (V_i = 5.40 ± 0.23 nmol min^{-1} μg^{-1}) indicated that, at high PS concentrations, the rate became 2.8 times slower than the maximum rate exhibited by the enzyme. It was also observed that *Mma*SerB2 showed no significant cooperativity in substrate binding (n = 1.1 ± 0.1) but was cooperatively inhibited by PS at 4.4-fold K_M concentrations (K_i = 4.32 ± 0.21 mM). Compared to Grant's results, *Mma*SerB2 appeared to be more sensitive to substrate inhibition than *Mtb*SerB2 (K_i = 23 ± 5 mM [34]).

Enzyme	**Work**	**K_M (µM)**	**V_{max} (nmol min^{-1} μg^{-1})**	**k_{cat} (s^{-1})**	**k_{cat}/K_M (10^4 $M^{-1}s^{-1}$)**
***Mma*SerB2**	Our group	985 ± 128	15.3 ± 1.3	11.7 ± 0.9	1.19
***Mtb*SerB2**	Our group [24]	195 ± 4	15.4 ± 0.1	11.2 ± 0.1	5.72
	Grant [34]	380 ± 50	-	18.6 ± 1.1	4.9

Globally, this kinetic behavior is typical of a multisite (homodimeric) enzyme inhibited by saturating concentrations of its substrate [36]. The shape of the curve indicates that *Mma*SerB2 is more catalytically active when only one of its two active sites is occupied by PS (low concentrations). At high PS concentrations, the velocity decreases as a major fraction of the enzyme is converted to the less active doubly occupied *Mma*SerB2. Furthermore, it would be possible that PS also interacts at an allosteric site. Such an inhibitory site could be found at the interface of ACT1 and ACT2 domains, where L-serine is known to bind and exert a regulatory effect in *Mtb*SerB2 and *Mtb*PGDH [34,37]. This hypothesis is further supported by the fact that *Mtb*SerB2 mutant G18A/G108A presents no substrate inhibition, as shown by Grant [34]. The two glycine residues are, indeed, required for efficient L-serine binding in ACT domains [22,31]. If PS can also interact at this site, mutation G18A/G108A in *Mtb*SerB2 would, as observed, prevent the binding event and hence substrate inhibition. A docking experiment using Glide (Schrödinger, LLC, New York) confirmed that PS fits in the L-serine binding site of *Mma*SerB2 model and could interact with the orthologous G20 residue, as well as with D17, T22, and I126 (**Figure S2**).

Inhibition of the phosphatase activity of *Mma*SerB2 by CFZ and harmine derivatives

The effect of CFZ and our previously described trisubstituted harmine derivatives [24] (**Figure S3**) was tested on *Mma*SerB2 phosphatase activity. As shown in **Figure 3E**, compounds **91, 95,** and **124** almost completely abolished enzyme activity at 10 µM. The effect was observed to the same extent for the three inhibitors. On the other hand, CFZ and derivative **88** had little effect at 10 µM. However, we observed a significant reduction in phosphatase activity when the inhibitors concentration was increased to 100 µM in the assay. In these conditions, the residual activity dropped to 2.3% in the case of CFZ and to 20% for the slightly less potent compound **88**. These results show that all five compounds have also

an inhibitory effect on *Mma*SerB2 and the trend was in good agreement with that observed for *Mtb*SerB2 [21,24].

CONCLUSION

The results of this work support that, like *Mtb*SerB2, *Mma*SerB2 is a Mg^{2+}-dependent, mesophilic HAD-like phosphatase that is most active near neutral pH. With the two orthologues sharing a very high sequence similarity and an almost identical architecture, as predicted by homology modeling, these results could be expected. Both PSPs are inhibited by their substrate, *O*-phospho-L-serine, and the kinetic behavior of *Mma*SerB2 was shown to be consistent with a mechanism of partial uncompetitive substrate inhibition that supports the homodimer model. The mechanism could also involve the interaction of PS at the ACT domains interface. While they showed comparable maximal catalytic rate and affinity for PS, *Mma*SerB2 was more sensitive to substrate inhibition (lower K_i) than *Mtb*SerB2. Finally, this work led to the identification of clofazimine and trisubstituted harmine derivatives as inhibitors of *Mma*SerB2 phosphatase activity.

ACKNOWLEDGEMENTS

The authors would like to thank Adrien Lesne for his valuable contribution to the experiments. The pAVA0421-*serb2* plasmid was generously provided by the Seattle Structural Genomics Center for Infectious Disease (www.SSGCID.org) which is supported by Federal Contract No. HHSN272201700059C from the National Institute of Allergy and Infectious Diseases, National Institutes of Health, Department of Health and Human Services.

FUNDING

EP acknowledges the Fonds de la Recherche Scientifique (F.R.S.-FNRS, Belgium) for her Research Fellow grant.

REFERENCES

[1] S.J. Gluckman, Mycobacterium marinum, Clin. Dermatol. 13 (1995) 273–276. https://doi.org/10.1016/0738-081X(95)00023-9.

[2] D.E. Reavill, R.E. Schmidt, Mycobacterial lesions in fish, amphibians, reptiles, rodents, lagomorphs, and ferrets with reference to animal models, Vet. Clin. North Am. Pract. 15 (2012) 25-40.

[3] F. Linell, A. Norden, Mycobacterium balnei, A New Acid-Fast Bacillus occurring in Swimming Pools and Capable of producing Skin Lesions in Humans., Acta Tuberc. Scand. (1954) 84.

[4] M.A. Bhatty, D.P. Turner, S.T. Chamberlain, Mycobacterium marinum hand infection: case reports and review of literature, Br. J. Plast. Surg. 53 (2000) 161–165.

[5] J.A. Jernigan, B.M. Farr, Incubation Period and Sources of Exposure for Cutaneous Mycobacterium marinum Infection: Case Report and Review of the Literature, Clin. Infect. Dis. 31 (2000) 439–443.

[6] P. Ang, N. Rattana-Apiromyakij, C.L. Goh, Retrospective study of Mycobacterium marinum skin infections, Int. J. Dermatol. 39 (2000) 343–347. https://doi.org/10.1046/j.1365-4362.2000.00916.x.

[7] T. Mason, K. Snell, E. Mittge, E. Melancon, R. Montgomery, M. McFadden, J. Camoriano, M.L. Kent, C.M. Whipps, J. Peirce, Strategies to Mitigate a Mycobacterium marinum Outbreak in a Zebrafish Research Facility, Zebrafish. 13 (2016) S77–S87. https://doi.org/10.1089/zeb.2015.1218.

[8] T. Tønjum, D.B. Welty, E. Jantzen, P.L. Small, Differentiation of Mycobacterium ulcerans, M. marinum, and M. haemophilum: Mapping of their relationships to M.

tuberculosis by fatty acid profile analysis, DNA-DNA hybridization, and 16s rRNA gene sequence analysis, J. Clin. Microbiol. 36 (1998) 918–925. https://doi.org/10.1128/jcm.36.4.918-925.1998.

[9] H. Tükenmez, I. Edström, R. Ummanni, S.B. Fick, C. Sundin, M. Elofsson, C. Larsson, Mycobacterium tuberculosis virulence inhibitors discovered by Mycobacterium marinum high-throughput screening, Sci. Rep. 9 (2019) 1–9. https://doi.org/10.1038/s41598-018-37176-4.

[10] C.L. Cosma, K. Klein, R. Kim, D. Beery, L. Ramakrishnan, Mycobacterium marinum Erp is a virulence determinant required for cell wall integrity and intracellular survival, Infect. Immun. 74 (2006) 3125–3133. https://doi.org/10.1128/IAI.02061-05.

[11] L. Ramakrishnan, S. Falkow, Mycobacterium marinum persists in cultured mammalian cells in a temperature-restricted fashion, Infect. Immun. 62 (1994) 3222–3229. https://doi.org/10.1128/iai.62.8.3222-3229.1994.

[12] C.L. Cosma, D.R. Sherman, L. Ramakrishnan, The Secret Lives of the Pathogenic Mycobacteria, Annu. Rev. Microbiol. 57 (2003) 641–676. https://doi.org/10.1146/annurev.micro.57.030502.091033.

[13] T.P. Stinear, T. Seemann, P.F. Harrison, G.A. Jenkin, J.K. Davies, P.D.R. Johnson, Z. Abdellah, C. Arrowsmith, T. Chillingworth, C. Churcher, K. Clarke, A. Cronin, P. Davis, I. Goodhead, N. Holroyd, K. Jagels, A. Lord, S. Moule, K. Mungall, H. Norbertczak, M.A. Quail, E. Rabbinowitsch, D. Walker, B. White, S. Whitehead, P.L.C. Small, R. Brosch, L. Ramakrishnan, M.A. Fischbach, J. Parkhill, S.T. Cole, Insights from the complete genome sequence of Mycobacterium marinum on the evolution of Mycobacterium tuberculosis, Genome Res. 18 (2008) 729–741. https://doi.org/10.1101/gr.075069.107.

[14] D.M. Tobin, L. Ramakrishnan, Comparative pathogenesis of Mycobacterium marinum and Mycobacterium tuberculosis, Cell. Microbiol. 10 (2008) 1027–1039. https://doi.org/10.1111/j.1462-5822.2008.01133.x.

[15] L. Ramakrishnan, Using Mycobacterium marinum and its hosts to study tuberculosis, Curr. Sci. 86 (2004) 82–92.

[16] A. Ichihara, D.M. Greenberg, Further studies on the pathway of serine formation from carbohydrate, J. Biol. Chem. 224 (1956) 331–340.

[17] H.E. Umbarger, M.A. Umbarger, P.M.L. Siu, Biosynthesis of serine in Escherichia coli and Salmonella typhimurium, J. Bacteriol. 85 (1963) 1431–1439.

[18] C.M. Sassetti, D.H. Boyd, E.J. Rubin, Genes required for mycobacterial growth defined by high density mutagenesis, Mol. Microbiol. 48 (2003) 77–84. https://doi.org/10.1046/j.1365-2958.2003.03425.x.

[19] S. Cole, R. Brosch, J. Parkhill, T. Garnier, C. Churcher, D. Harris, S. Gordon, K. Eiglmeier, B. Barrell, Deciphering the biology of Mycobacterium tuberculosis from the complete genome sequence, Nature. 393 (1998) 537–544. https://doi.org/10.1038/29241.

[20] M. Haufroid, J. Wouters, Targeting the Serine Pathway : A Promising Approach against Tuberculosis ?, (2019) 1–20. https://doi.org/10.3390/ph12020066.

[21] S. Shree, A.K. Singh, R. Saxena, H. Kumar, A. Agarwal, V.K. Sharma, K. Srivastava, K.K. Srivastava, S. Sanyal, R. Ramachandran, The M. tuberculosis HAD phosphatase (Rv3042c) interacts with host proteins and is inhibited by Clofazimine, Cell. Mol. Life Sci. 73 (2016) 3401–3417. https://doi.org/10.1007/s00018-016-2177-2.

[22] G.P. Yadav, S. Shree, R. Maurya, N. Rai, D.K. Singh, K.K. Srivastava, R.

Ramachandran, Characterization of M. tuberculosis SerB2, an essential HAD-family phosphatase, reveals novel properties, PLoS One. 9 (2014) 1–24. https://doi.org/10.1371/journal.pone.0115409.

[23] G. Arora, P. Tiwari, R.S. Mandal, A. Gupta, D. Sharma, S. Saha, R. Singh, High throughput screen identifies small molecule inhibitors specific for Mycobacterium tuberculosis phosphoserine phosphatase, J. Biol. Chem. 289 (2014) 25149–25165. https://doi.org/10.1074/jbc.M114.597682.

[24] E. Pierson, M. Haufroid, T.P. Gosain, P. Chopra, R. Singh, J. Wouters, Identification and Repurposing of Trisubstituted Harmine Derivatives as Novel Inhibitors of Mycobacterium tuberculosis Phosphoserine Phosphatase, Molecules. 25 (2020) 1–17. https://doi.org/10.3390/molecules25020415.

[25] F. Corpet, Multiple sequence alignment with hierarchical clustering, Nucleic Acids Res. 16 (1988) 10881–10890.

[26] X. Robert, P. Gouet, Deciphering key features in protein structures with the new ENDscript server, Nucleic Acids Res. 42 (2014) 320–324. https://doi.org/10.1093/nar/gku316.

[27] P. Stothard, The Sequence Manipulation Suite: JavaScript programs for analyzing and formatting protein and DNA sequences, Biotechniques. 28 (2000) 1102–1104.

[28] V.J. LiCata, N.M. Allewell, Is substrate inhibition a consequence of allostery in aspartate transcarbamylase?, Biophys. Chem. 64 (1997) 225–234. https://doi.org/10.1016/S0301-4622(96)02204-1.

[29] E.M. Weerdenburg, A.M. Abdallah, F. Rangkuti, M.A. El Ghany, T.D. Otto, S.A. Adroub, D. Molenaar, R. Ummels, K. ter Veen, G. van Stempvoort, A.M. van der Sar,

S. Ali, G.C. Langridge, N.R. Thomson, A. Pain, W. Bitter, Genome-wide transposon mutagenesis indicates that Mycobacterium marinum customizes its virulence mechanisms for survival and replication in different hosts, Infect. Immun. 83 (2015) 1778–1788. https://doi.org/10.1128/IAI.03050-14.

[30] D.M. Chipman, B. Shaanan, The ACT domain family, Curr. Opin. Struct. Biol. 11 (2001) 694–700. https://doi.org/10.1016/S0959-440X(01)00272-X.

[31] G.A. Grant, The ACT domain: A small molecule binding domain and its role as a common regulatory element, J. Biol. Chem. 281 (2006) 33825–33829. https://doi.org/10.1074/jbc.R600024200.

[32] A. Seifried, J. Schultz, A. Gohla, Human HAD phosphatases: Structure, mechanism, and roles in health and disease, FEBS J. 280 (2013) 549–571. https://doi.org/10.1111/j.1742-4658.2012.08633.x.

[33] A.M. Burroughs, K.N. Allen, D. Dunaway-Mariano, L. Aravind, Evolutionary Genomics of the HAD Superfamily: Understanding the Structural Adaptations and Catalytic Diversity in a Superfamily of Phosphoesterases and Allied Enzymes, J. Mol. Biol. 361 (2006) 1003–1034. https://doi.org/10.1016/j.jmb.2006.06.049.

[34] G.A. Grant, Regulatory Mechanism of Mycobacterium tuberculosis Phosphoserine Phosphatase SerB2, Biochemistry. 56 (2017) 6481–6490. https://doi.org/10.1021/acs.biochem.7b01082.

[35] A. Waterhouse, M. Bertoni, S. Bienert, G. Studer, G. Tauriello, R. Gumienny, F.T. Heer, T.A.P. De Beer, C. Rempfer, L. Bordoli, R. Lepore, T. Schwede, SWISS-MODEL: Homology modelling of protein structures and complexes, Nucleic Acids Res. 46 (2018) W296–W303. https://doi.org/10.1093/nar/gky427.

[36] I. Segel, Multisite and allosteric enzymes, in: Enzyme Kinetics: Behavior and Analysis of Rapid Equilibrium and Steady-State Enzyme Systems, John Wiley & Sons: Hoboken, NJ, USA, 1993: pp. 346–464.

[37] D.J. Schuller, G.A. Grant, L.J. Banaszak, The allosteric ligand site in the Vmax-type cooperative enzyme phosphoglycerate dehydrogenase, Nat. Struct. Biol. 2 (1995) 69–76.

FIGURES/TABLES LEGENDS

Table 1. Kinetic parameters of *Mma*SerB2 and *Mtb*SerB2 for the dephosphorylation of *O*-phospho-L-serine.

Figure 1. Multiple sequence alignment of *M. marinum* SerB2 (Uniprot: B2HHH0) ; *M. tuberculosis* SerB2 (Uniprot: O53289) ; *M. avium* SerB (PDB: 3P96) and *H. sapiens* PSP (Uniprot: P78330). The secondary structure elements of *Mav*SerB are shown in the first line. Strictly conserved residues are highlighted in red and highly conserved residues are shown in red font. ACT1/ACT2 and C1 cap module domains are boxed in cyan and grey respectively. Motifs 1 (hhhDxDxT(L/V)h), 2 (hh(S/T)), 3 and 4 ($K_{18\text{-}30}$(G/S)(D/N)$x_{3\text{-}4}$(D/E)), where h is an hydrophobic residue and x is any residue, are boxed in dark blue. Residues important for L-serine binding in *Mtb*SerB2 and *Mav*SerB are boxed in black.

Figure 2. A) Structure of *Mma*SerB2 modeled by homology on the basis of *M. avium* SerB structure (PDB 3P96). The individual domains are labelled. Active site residues are shown in red. Residues predicted to be important for L-serine binding are labelled and shown in pink. **B)** Homodimeric assembly of homology-modeled *Mma*SerB2. The second monomer is shown in orange. One of the two predicted L-Ser binding sites at the interface of ACT1 and ACT2 domains is circled.

Figure 3. Effect of selected reaction conditions on *Mma*SerB2 phosphatase activity during the dephosphorylation of *O*-phospho-L-serine (PS). Data depicted are averaged from three independent experiments ± S.E. **A)** Influence of selected metal cations. **B)** Influence of the reaction buffer pH. **C)** Influence of the reaction temperature. **D)** Variation of the initial velocity as a function of PS concentration. Best fit of **equation (1)** is shown as a solid line. **E)** Influence of Clofazimine (CFZ) and trisubstituted harmine derivatives (**88, 95, 91,** and **124**) in presence of 2% DMSO. The activity of MmaSerB2 in presence of 2% DMSO and no inhibitor (DMSO condition) was defined as 100% activity.

FIGURES

Figure 1

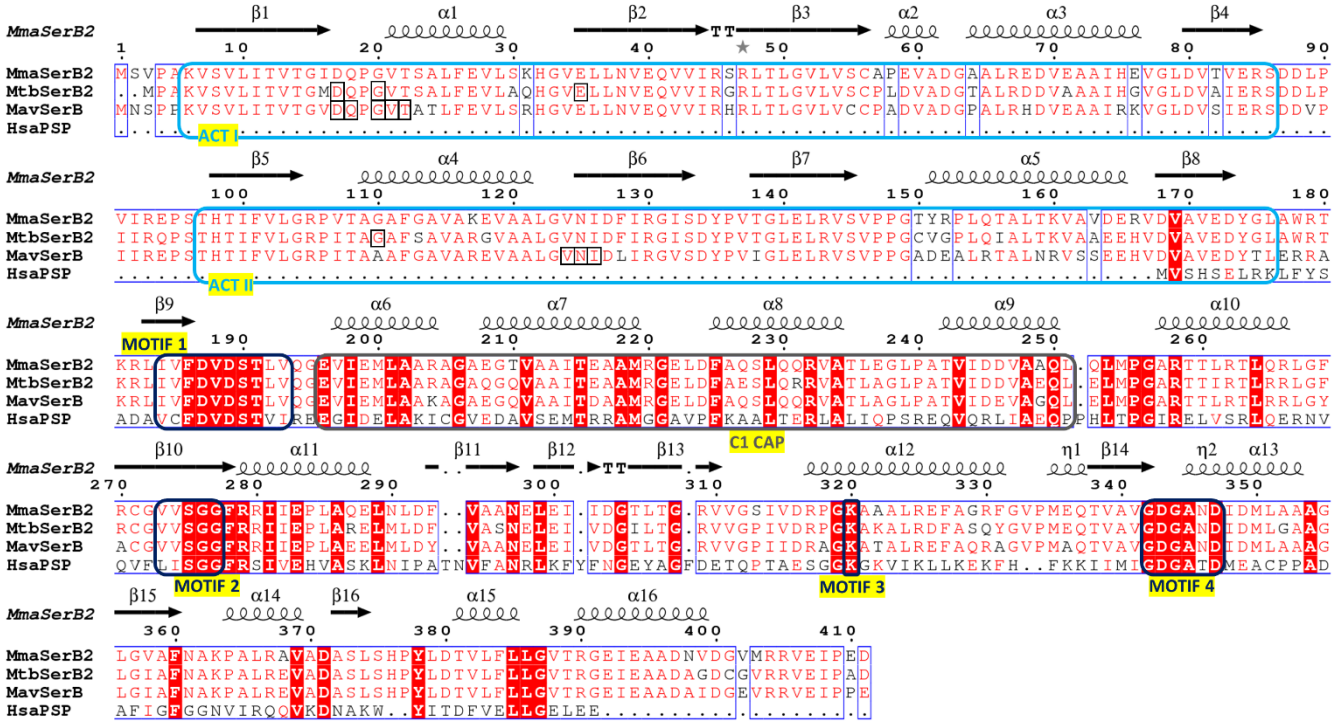

Figure 2

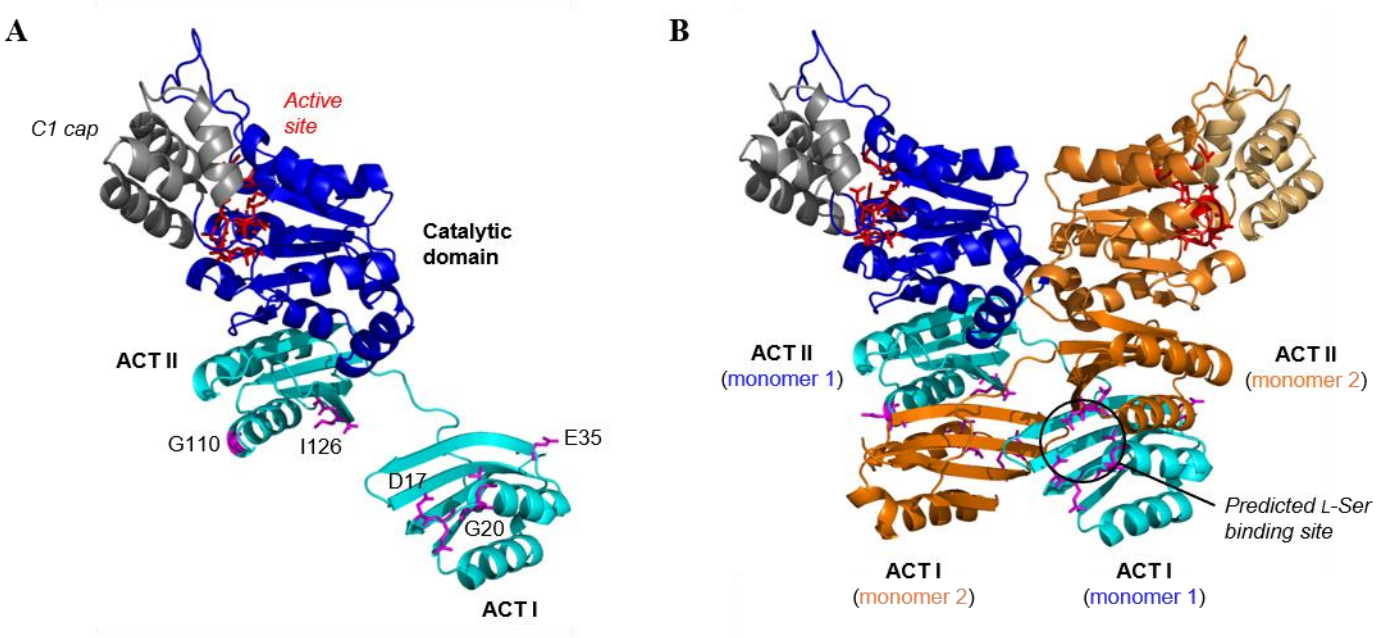

Figure 3

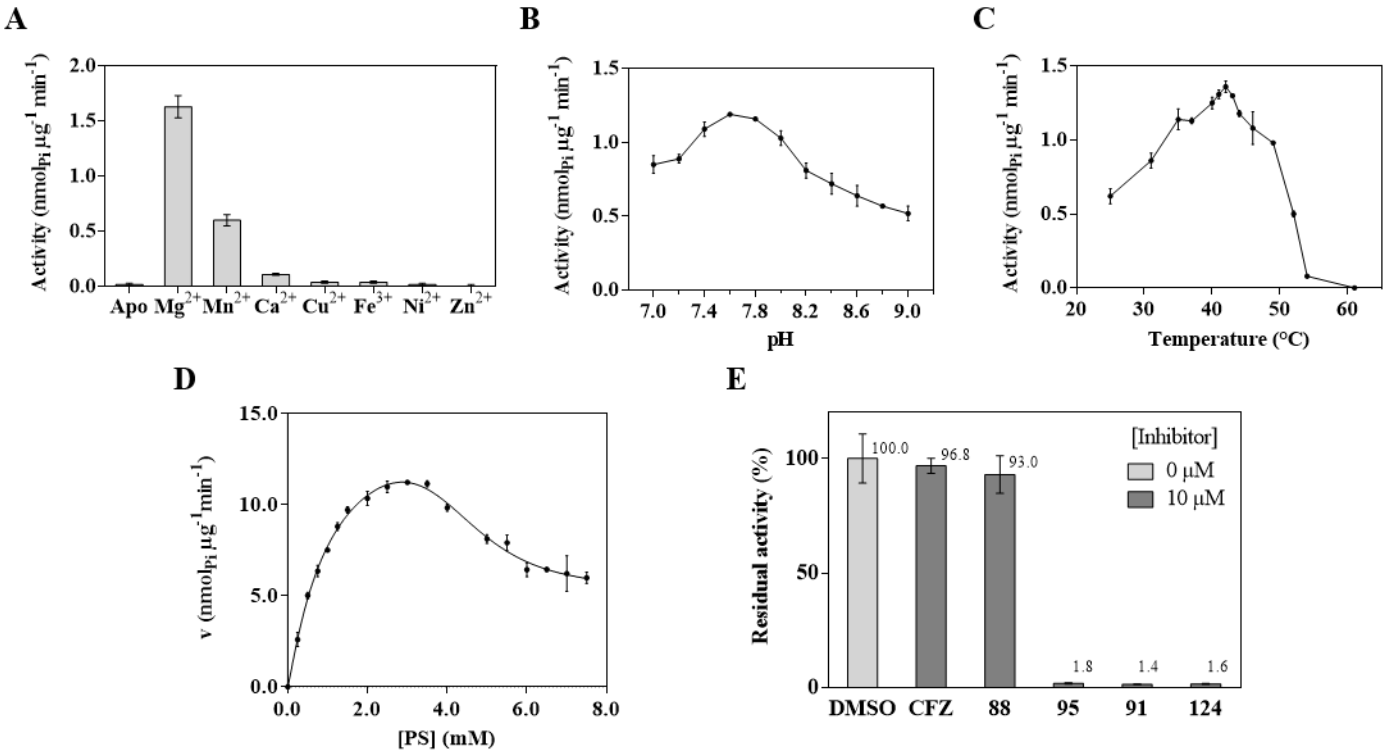

SUPPLEMENTARY MATERIAL

see uploaded file SUPPLEMENTARY_DATA.docx